CS 229 FINAL PROJECT: STRUCTURE PREDICTION OF OPTICAL FUNCTIONAL DEVICES WITH DEEP LEARNING

KAI ZHANG, SHIYU LIU, AND QING WANG

Nomenclature

$\boldsymbol{x}$	The output electrical field, which is the input to the neural networks
$\boldsymbol{y}$	The Si structure, which is the output of the neural networks
H_l	Number of neurons in in layer l
m	Size of data sets
n	Size of the Si structure
p	Number of layers in the neural networks
r	Size of the discretized electrical field signal

1. Introduction

Improving the efficiency of optical device is important in a variety of applications. However, this process is typically done empirically. In this project, we formulate a systematically way to improve the efficiency of optical device design with machine learning.

The optical device we focus on is a silicon (Si) nano-structure. This device is constructed by a series of Si nano-cells, which is represented as the $\{0, 1\}$ binary series in Fig. 1. In Fig. 1, 1 and 0 indicate the existence and void of Si at a particular location. A beam of light perpendicular to the Si structure is incident onto the Si structure and excites the surrounding electric field. In this project, we use the output electric field to predict its corresponding Si structure.

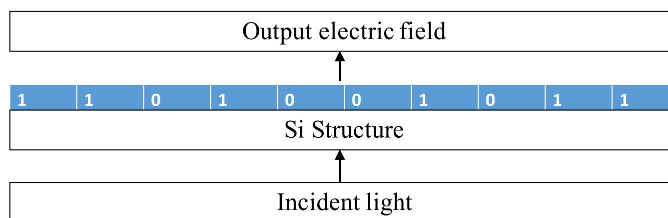

Figure 1. Schematic of 1D Si structure with simulation procedure.

Note that the projection from the input Si structure to the output electrical field follows the underlying physical law governed by the Maxwell's equations, which is a full rank operation, the inversion of this problem is well defined. Therefore, with appropriate machine learning technique, we can predict the Si structure based on the output electrical field.

To address the non-linear relation between the Si structure and the output electrical field, we use deep learning as our training algorithm. In the meanwhile, this approach also allows us to reduce the dimensionality of the underlying physics. One the other hand, although the Si structure that is represented by an $\mathbb{R}^{1\times n}$ vector can take 2^n combinations, a functional optical device almost always follows specific patterns and the number of output labels in the neural networks is confined. Therefore, by limiting our scope to

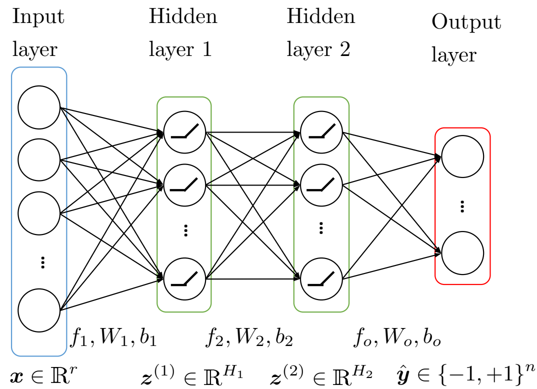

FIGURE 2. Neural networks with 2 hidden layers.

Si structures with physical functionalities, we can get a converged solution using finite number of data sets.

The structure of this report is given as follows. A detailed interpretation of the neural networks we use in this project is provided in Section 2. Section 3 describes the procedure of the simulation and the preprocessing of the training data. The training results are discussed in Section 4.

2. NEURAL NETWORKS

In deep learning, the input data is processed through a neural networks that is constructed by a multiple layers of computational units. An example of a four-layer neural networks is shown in Fig. 2. This neural networks consists of one input layer, one output layer and two hidden layers. Data propagates from the input layer to the output layer by going through transformation functions between each layer. The dimensions of hidden layers determine the complexity of parameterization of the neural networks.

The propagation of data in the neural networks is characterized by a forward-feeding process. Specifically, each layer takes a linear transformation of the data from previous layer and process it using an activation function. At layer l, we can express the forward-feeding process as:

$$\boldsymbol{z}^{(l)} = f_l\left(W_l \boldsymbol{z}^{(l-1)} + \boldsymbol{b}_l\right), \forall l \in \{1, ..., p\}, \tag{1}$$

where $\boldsymbol{z}_l$ is the transformed data, W_l and b_l are the weights and bias respectively, and f_l is the activation function at layer l. In the first hidden layer, the input data $\boldsymbol{z}^{(0)} = \boldsymbol{x}$, which is the input to the neural networks. For layers with size of H_l, we have $W_l \in \mathbb{R}^{H_l \times H_{l-1}}$ and $\boldsymbol{b}_l \in \mathbb{R}^{1 \times H_l}$. In addition, in this project, we use a rectified linear unit (ReLU) function as the activation function at all layers, which is defined as:

$$f_l(z) = \max(0, z), \forall l \in \{1, ..., p\}, \tag{2}$$

where p is the total number of layers in the neural networks.

The network between the last hidden layer and the output layer gives the prediction to the output data. Because the output data is a vector of size n, we represent the prediction function by a linear transformation, which is:

$$\hat{\boldsymbol{y}} = W_o \boldsymbol{z}^{(p)} + \boldsymbol{b}_o. \tag{3}$$

Because the output vector in this project is binary, we obtain our predictions as:

$$\hat{\hat{y}}_j = \begin{cases} +1, & \hat{y}_j > 0 \\ -1, & \hat{y}_j \leq 0. \end{cases} \tag{4}$$

The cost function of this neural networks is defined by a mean square error (MSE) function, which is:

$$J(W, b; \boldsymbol{x}, \boldsymbol{y}) = \frac{1}{m} \sum_{i=1}^{m} \|\boldsymbol{y}^{(i)} - \hat{\boldsymbol{y}}^{(i)}\|_2^2. \tag{5}$$

Because $J(W, b; \boldsymbol{x}, \boldsymbol{y})$ is convex, the parameters can be trained by solving the following problem:

$$\min_{W_l, b_l, l=\{1,\ldots,p\}} J(W, b; \boldsymbol{x}, \boldsymbol{y}). \tag{6}$$

We solve this problem using stochastic gradient descent in a set of back-propagation steps.

The training and testing errors are defined by the following equation:

$$\epsilon_{\text{train/test}} = \sqrt{\frac{\sum_{i=1}^{m} \|\hat{\boldsymbol{y}}^{(i)} - \boldsymbol{y}^{(i)}\|_2^2}{\sum_{i=1}^{m} \|\boldsymbol{y}^{(i)}\|_2^2}}. \tag{7}$$

This error definition is used to characterize the convergence of the learning process at each iteration. In addition, to quantify the accuracy in Si structure prediction, we define the prediction error as:

$$\epsilon_{\text{prediction}} = \frac{1}{m} \sum_{i=1}^{m} \frac{\sum_{j=1}^{n} \mathbb{1}\{\hat{\bar{y}}_j \neq y_j\}}{n}. \tag{8}$$

We use this error definition as a metric to the performance of the learning algorithm.

3. Problem setup and data acquisition

We obtain the data for learning from simulations of the optic-electric interaction using the rigorous coupled-wave analysis (RCWA) software. In the simulations, the refraction index of Si is $n_{Si} = 3.5$ and the refraction index of vacuum is $n_{vacuum} = 1$. Light with wavelength $\lambda = 1\ \mu m$ is illuminated perpendicular to the Si structure from the top. For each Si structure randomly generated by the RCWA software, the corresponding electric field is recorded. Figures 3(a) and 3(b) show an example of the Si structure and the magnitude of its output electric field. The Si structure is represented by the dark red and vacuum is represented by dark blue in Fig. 3(a). In Fig. 3(b), the electric field above the Si structure is activated by the reflected light and the electric field below the Si structure is activated by the transmitted light.

For the learning purpose, we collected 250000 data sets from the simulations. We use 80% of the data sets as the training set and the rest of the 20% as the test set. The inputs of learning are the electric fields retrieved at two specific vertical locations, which are represented by $\boldsymbol{x'}^{(i)} \in \mathbb{C}^{1\times 51}$. In the first case, the inputs are taken at the near field that is 0.1λ below the Si structure; in the second case, the inputs are taken at the far field that is 10λ below the Si struture. Note that $\boldsymbol{x'}$ is complex because the electric field signal contains both magnitude and phase information. To avoid the computations with complex numbers, we treat the magnitude and phase of the inputs separately. Therefore, the inputs used in the learning process are represented by $\boldsymbol{x}^{(i)} \in \mathbb{R}^{1\times 102}$. The outputs of learning are the binary vector of Si structure, which is $\boldsymbol{y}^{(i)} \in \{+1, -1\}^n$, where $n = 20$ is used.

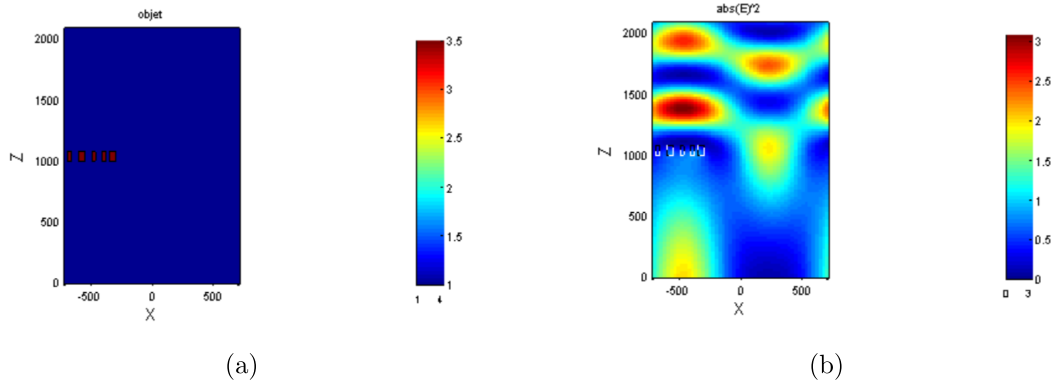

FIGURE 3. (a) 1D Si structure aligned along x-direction at height $z = 1000$; and (b) the corresponding output electric field given light normal incident on Si structures.

4. TRAINING OUTCOME AND DISCUSSION

The training curve for the near field and far field learning are shown in Figs. 4(a) and 4(b). In both cases, the results converges in about 100 iterations. The test error is slightly greater than the training error. However, the errors for the near-field learning, which are 34.9% for training and 35.4% for testing, are more than two-folds lower than the errors for the far-field training, which are 86.8% for training and 86.9% for testing. The corresponding prediction error for the near-field learning are 3.5% for training and 3.6% for testing, and the prediction error for far-field learning are 29.5% for training and 29.6% for testing. The degradation in performance as the data collection location moves away from the Si structure is a consequence of the decay in optical intensity of the transmitted light. Information carried by the transmitted light dissipates as the light travels. This indicates that the electric field in the near-field provides a better metric than in the far-field to characterize the Si structure.

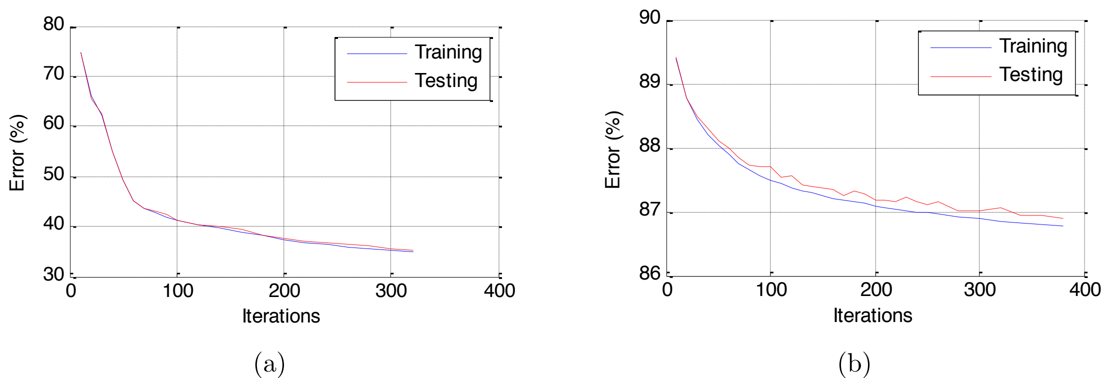

FIGURE 4. Learning curve with two-layer neural networks for: (a) near-field electric field training; (b) far-field electric field training.

To quantify the far-field efficiency of the prediction, we pre-define an output electric field and apply the parameters obtained from the far-field learning to predict its corresponding Si structure. The comparison of the far-field efficiency of the 45° transmitted light between the predicted Si structure and the optimal structure are shown in Fig. 5. Mispredictions in magnitude and phase of the electric field are observed in Fig. 5. The

efficiency associated with the predicted Si structure is 43.4%. To correct for potentially misrepresented Si cell in the predicted structure, we perform a local found method that alters each element in the predicted Si structure one at a time. With this approach, the efficiency improves to 51.2%. Note that the maximum efficiency for all possible 20-cell Si structures is 69.0%. This shows that the deep learning procedure provides us a reliable method to predict the Si structure for prescribed electric field.

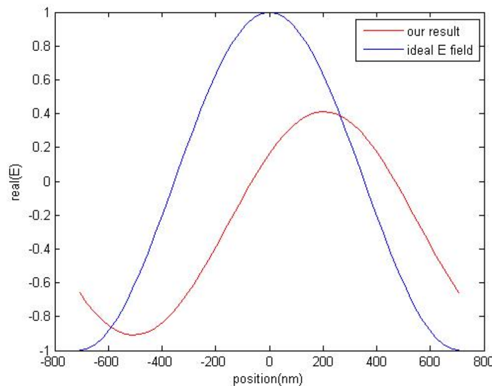

FIGURE 5. Comparison of 45° deflected transmitted light electric field of the predicted Si structure and the ideal 100% efficiency electric field.

5. CONCLUSION

In this project, we implemented a two-layer neural networks algorithm to study the relation between optical Si structures and the output electric fields. We trained two neural networks using the near-field and far-field electric field data obtained from the RCWA software. The size of the data sets used for learning is 250000. In both setups, the results converges in 100 iterations. The accuracy of prediction using the near-field data reached 96.5% and the accuracy using far-field data is 70.4%. With local found method, an efficiency of 51.2% is achieved by the predicted Si structure against the 69.0% maximum possible efficiency for the 45° transmitted-light. Compared to the traditional optical-device design process, the deep learning approach significantly improves the effectiveness of this process without considering the convoluted underlying physics.

To further improve the method, in our future research, we will test different cost functions for training such that the binary nature of the Si structure is better represented. The depth of the neural networks and the dimension of parameters will also be adjusted to optimize the results.